SEMARAK ILMU PUBLISHING

CFD Letters

Journal homepage:
https://semarakilmu.com.my/journals/index.php/CFD_Letters/index
ISSN: 2180-1363

Aerodynamic Performance Enhancement of a Heavy Trucks using Experimental and Computational Investigation

Mohamed B. Farghaly[1,*], H. H. Sarhan[2], E. S. Abdelghany[3]

[1] Department of Mechanical Engineering, Faculty of Engineering, Fayoum University, 63514, Fayoum, Egypt
[2] Mechanical Engineering Department, Faculty of Engineering, Port Said University, Port Said, Egypt
[3] Department of Mechanical Engineering, Faculty of Engineering, Albaha University KSA, on Leave from Institute of Aviation Engineering and Technology, Giza, Egypt

ARTICLE INFO

Article history:
Received 1 January 2023
Received in revised form 3 February 2023
Accepted 2 March 2023
Available online 1 August 2023

Keywords:
Aerodynamics; Computational fluid dynamics; Drag reduction devices; Truck–Cabin profiles; Wind tunnel test

ABSTRACT

Improving the aerodynamic performance of a heavy vehicles is one of the essential issues used in automotive industry to reduce the fuel consumption. In this work, various drag reduction devices were added to improve the vehicle profiles and the effects of each device were experimentally and computationally investigated. These additional devices are Cap of truck with different angle, Gap device with different length and Flat Flap with different angle and dimensions. 1/50th scale of a standard heavy truck were taken to construct the computational and experimental model. The drag coefficient, contours of turbulence kinetic energy, pressure, velocity, streamlines, velocity vectors were predicted with and without additional devices. The obtained results show that these attached devices have a notable impact on the aerodynamic drag reduction of the heavy vehicles and trucks. Installing all supplementary parts at the same time help to reduce the drag coefficient by about 59 % compared with the truck without any profile's modifications. Finally, the experimental results show good agreement with the computational results with acceptable percentage error of about 5%.

1. Introduction

The aerodynamic shapes of heavy freight vehicles are inefficient compared with the on-ground vehicles because of their bluff shape of bodies and larger frontal area. Reducing the aerodynamic profile drag is considered one of the most important objectives in several automotive development researches aiming to energy save, reduce the emissions, and hence protecting the environment from the danger of global warming. In the heavy freight vehicles, improving the aerodynamic efficiency are one of the most important factors that used to enhance the driving control performance, decrease the fuel consumption, reduce the carbon emissions of petroleum fuels usage. Also, the aerodynamically refined shapes are aesthetically attractive and can help to increase the freight capacity of vehicles. The road vehicles are consumed more than 1.3 trillion litres of diesel and petrol,

* *Corresponding author.*
E-mail address: mbs12@fayoum.edu.eg (Mohamed B. Farghaly)

https://doi.org/10.37934/cfdl.15.8.7394

this is causing a high level of pollution (CO_2) due to burning this fossil fuels [1, 2]. The calculation method of the specific exhaust emissions for a compression ignition (C.I) engine fuelled by palm biodiesel blend was proposed by Sarwani *et al.,* [3] and the percentage of volumetric emission into specific emission (g/km) was investigated. The effect of vacuum insulation panels (VIPs) was studied to reduce consumption of fuel in transportation systems for cold storage trucks [4].

To improve and development the final product, in recent years the industry of heavy truck has focused mainly on the fuel efficiency due to some important parameters such as increasing restriction of emissions regulations, fuel price rise, and finally the operational costs optimization of the heavy trucks. Although the significant growth and development in the aerodynamic shapes of sport and passenger cars, but the heavy freight vehicles aerodynamic design still needs additional development to minimize fuel consumption. While the heavy freight vehicles involve just 4% of vehicles on-road, but they are accountable for over 20% of the transportation fuel consumption and carbon emissions [5]. The technical report National Research Council of Canada stated that a 20% reduction in the coefficient of drag can be able to increase about 10% in the fuel efficiency [6]. The relatively high value of the heavy freight vehicles main body drag coefficient are consider the major sources of low contributions of fuel economy for these vehicles. The range of main body drag coefficient are about 0.8 to 1.8 for heavy freight vehicles [7-10], compared to about 0.3 and 0.4 for a sedan and SUV respectively [11, 12]. Most energy of heavy freight vehicles is utilized to overcoming the aerodynamic drag of vehicle as accelerate, thus decreasing consumption of fuel of the heavy freight vehicles can be achieved by modifying the shapes of truck to reduce the air resistance.

An experimental study on a heavy truck was investigated to predict the fuel saving potentials due to drag reduction, the obtained results indicate that the aerodynamic drag is directly proportional to the square of the vehicles speed and the aerodynamic drag is considered the main fuel consumption source at the vehicles cruise speed, also 50% of the heavy truck power is required to overcome the aerodynamic drag at typical speed of about 90-100 km/h on highway road [13]. The gap effect between trailer and tractor on a general model of truck was investigated experimentally using wind tunnel test, the percentage improvement of the aerodynamic performance, economics, handling, safety of the trucks were determined by Englar & Robert J. [14]. The effect of yaw angles and fairings on the drag reduction were investigated experimentally on a $1/10^{th}$ scale model of semi-trailer truck using wind tunnel testes, the obtained results show that truck front area has most important effect on truck drag, which reduce the drag by about 26%, using cab roof fairing can be reduce the drag of truck by about 17%, joint cab roof fairing with tractor-trailer gap can be reduce the drag of truck by about 25.5% [15].

In past decades several experimental studies in both road test and wind tunnel lab have been performed to examine the flow behaviour around the heavy tractor-trailer. Recently, due to the growth of computing performances computational fluid dynamics (CFD) are becoming common for these simulations. The CFD has computational power available and meshes variety that can be able to simulate the complex geometry of any vehicle and the greatly transient of the behaviour of flow-field. To reduce the drag force and the fuel consumption by delay and control the flow separation, the airfoil of Boeing-737 with modified shape profile was studied numerically by Niknahad & Ali [16] and the results obtained show a significant decrease in the total drag force and consequently decrease in fuel consumption. The effect of passive control of flow separation of multi-element airfoil on the aerodynamic performance characteristics was studied computationally at low Reynolds number for different angles of attack, the results obtained show that the optimized configurations of the multi-element airfoil have better performance than the conventional airfoil especially at high-level of attack angles [17]. Multiple devices have installed on the truck body to decrease the aerodynamic drag of heavy freight vehicles [18, 19]. For example, a boat-tail plates were used to raise

the base pressure of trailer for both operation conditions of crosswind and quiescent [20, 21]. Also, the trailer skirts, the roof extenders, and tractor side were used to decrease the aerodynamic drag and enhance the consumption of fuel of the heavy trucks [22]. A numerical study on a heavy truck of 40-tons in weight and travelling at 60 mph was investigated to predict the fuel saving potentials due to drag reduction, the obtained results indicate that the heavy truck consumes around 34L of fuel to overcome the drag through a 100-mile highway-rod, and under the same operation condition an average car would consume about four-time less [23]. The effect of adding join devices such as cab vane corner, deflector, cab/trailer gap, front fairing, back vane, and base flap on heavy vehicle drag reduction were studied using computational fluid dynamic (CFD) analysis, the obtained results indicate that using all supplementary devices at their enhanced positions reduce about 41% of aerodynamic drag comparing to the simple model [24].

A computational simulation was investigated on a full-scale and model of Class-8 trucks equipped with devices of drag reduction, the obtained results were validated with experimental result and the effect of unsteady flows on the fuel reduced are also determined by Hyams *et al.,* [25]. The truck-trailer profile modification was analysed numerically to predict the aerodynamic drag and its effect on the fuel consumption, shear stress transportation turbulence model (SST) was used, the obtained results indicate that the modification profiles can be able to reduce the aerodynamic drag around 21%, which reduces the consumption of fuel by about 4L per 100km for truck of diesel-powered [26]. The effect of cabin profiles devices on the aerodynamic drag reduction were investigated computationally and experimentally on a $1/50^{th}$ scale model of semi-trailer truck using CFD analysis and wind tunnel testes, the obtained results indicate that the truck profile modifications have significant impact on drag reduction and using all drag reduction devices at their optimized positions and dimensions can be able to reduce the drag by about 36.03 % compared to the standard heavy-trucks without any modifications [27]. The influence of clearance gap size between trailer and tractor on the aerodynamic drag were investigated, the obtained results illustrate that the vehicle turning capacity is strongly affected in case of very small gap while, the vehicle tends to act as two separate bodies and produce twice drag in case of large gap, and in the case of cross-wind this effect may be amplified due to the relative yaw of vehicle relating to the free stream direction of wind [28].

Several analyses were investigated on a heavy truck aerodynamics combined with different drag reducing devices to predict the percentage in drag reduction, the obtained results indicate that using the side fairings and cab-roof fairings can be able to decrease the drag by about 9-17% [29-31], the trailer-front fairing can be able to decrease the drag by about 7-10% [32, 33], the side-skirts of both trailer and tractor can be able to decrease the drag by about 4-6% [34, 35], and the base flaps and boat-tail can be able to decrease the drag by about 7.5% [36].

A parametric analysis of a large vehicle travelling at speed of about 100km/h was studied by Khaled *et al.,* [37], the obtained results indicate that the vehicle consumes approximately about 53% of total fuel to deliver power to overcome aerodynamic drag. The average annual traveling distance of a heavy vehicle changes between 130000 km to 160000 km, due to such high traveling distance, any decrease in the aerodynamic drag will result a major fuel savings and decreases of greenhouse carbon gas emission, [38]. In the recent years various studies on the active devices of drag reduction such as suction of boundary layer were performed, but the need to provide energy and the complexity of their operation leads to did not allow to spread these devices in the markets. Another way that used to decrease the aerodynamic drag of heavy freight truck is platooning, but this technique needs a major change in the vehicle's infrastructure and driving behaviour, hence due to these purposes the platooning is not currently existing [39].

The novelty in this study is no major changes were performed on both infrastructure and body shape of the truck and the drag reduction devices were installed externally, and these devices are

simple and can be installed on the existing trucks with minimum cost and maximum benefit of fuel saving. In this work, various external devices of aerodynamic drag reduction were added to the existing shape profiles of a heavy truck aiming to improve the truck aerodynamic efficiency, decreasing the aerodynamic drag and fuel consumption, reduce the emissions, and hence, protecting the environment from the danger of global warming. The effects of each device on the drag reduction were experimentally and computationally investigated. These additional devices are Cap of truck with different angle, Gap device with different length and Flat Flap with different angle and dimensions. 1/50th scale of a standard heavy truck were taken to construct the computational and experimental models. The drag coefficient, contours of turbulence kinetic energy, velocity pressure, velocity vectors and streamlines were predicted with and without additional devices. The computational model was constructed by ANSYS FLUENT CFD software and the k-ω SST model of turbulence was used. The computational domain was solved for truck shape without and with different drag reduction devices and the obtained results are analysis and discussed.

2. Numerical Analysis

In this study, a one-fifty scale detailed model of a standard heavy-trucks is built to predict the truck drag experimentally and numerically. The aerodynamic impact of various drag reduction devices that added to the truck shape profile was investigated. These additional devices are the Cap of the truck with various angle, Gap device with various length and Flat Flap with various angle and dimensions. The detailed dimensions of the constructed truck model without any modification devices are illustrate in Figure 1. The computational model is solved using ANSYS FLUENT. The coefficient of drag, turbulence contours, pressure, temperature, velocity, streamlines, and vectors of velocity were investigated and discussed.

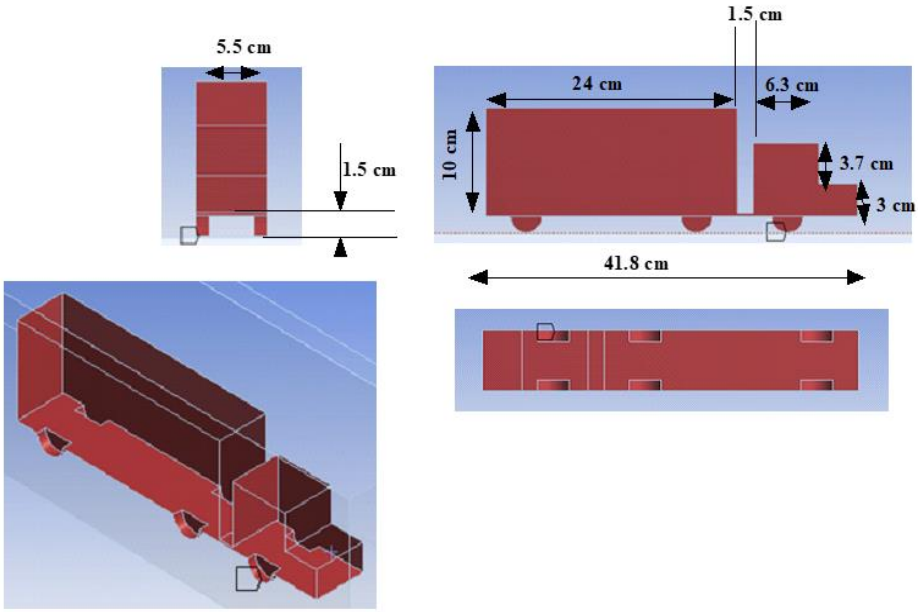

Fig. 1. Model of standard heavy truck with all dimensions

2.1 Mesh Setting and Boundary Conditions

To increase the calculation accuracy with time saving, the computational domain is modelled with two domains, one of them is internally and the other is externally as shown in Figure 2. The internal

domain has a dense and mesh with large nodes number and a small cells size, while the external domain has relatively less nodes and a large cells size. The boundary conditions are defined using DESIGN MODULAR program of ANSYS FLUENT. To validate the computational model, the same conditions of experimental work was selected and used later in wind tunnel test. The Reynolds number for the velocity inlet boundary (number 1) of about R_e = 5.75231x10^5. The air free stream temperature, pressure, viscosity, and density are 300K, 101325Pa, μ=1.7894×10^{-5}kg/m.s, and ρ=1.225kg/m^3, respectively. The pressure outlet (number 2) of about 101325Pa as the environmental pressure. The truck profile (number 3), the two vertical and horizontal planes around truck are considered adiabatic (with zero heat flux) and no-slip wall. A segregated-implicit solver of ANSYS FLUENT is used for velocity varying from 10m/s to 25m/s (R_e from 350000 to 650000).

To obtain accurately drag force calculation, grids near the truck body (internal domain) must be dense enough and computed fields must be large enough to balance accuracy versus calculation time of the solution. However, excessive fields and grids will cost too much computing resources and slow computing speed. Using unstructured tetrahedral mesh, rising mesh cells, but it is required supercomputer and additional time to solve the problem. Several researchers developed different methods and tools to overcome the described problems above. To construct great quality single and multi-block structure grid for complicated shape, several grid generation methods were presented [27, 40]. In the present study, the multi-block unstructured grid method was used to raise grids near the truck by creating block around the truck domain and making body inflation, as shown in Figure 3.

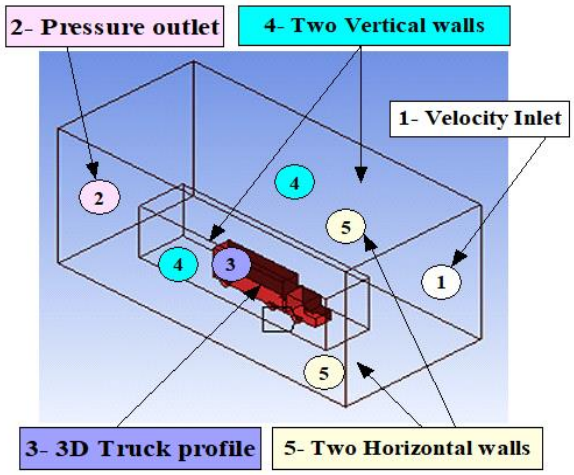

Fig. 2. Boundary conditions of a computational domain

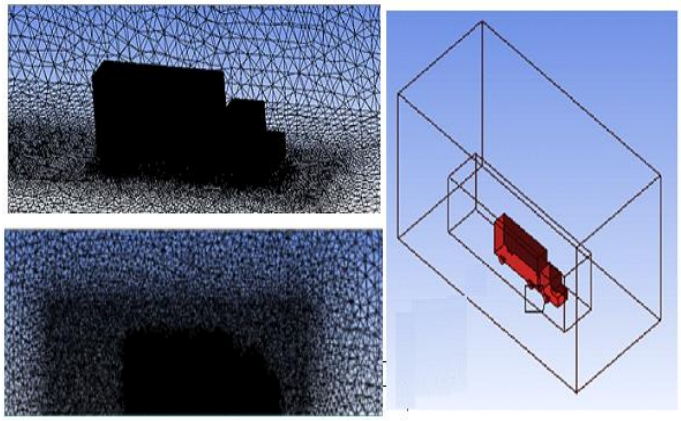

Fig. 3. Truck computational volume, (a) Mesh face sizing, (b) Multi block volume

2.2 Grid Dependencies Check and Verification

Generally, the numerical solution becomes high precise as more cells are used, but using extra cells also raises the computer memory and solution time required. The suitable nodes number was determined by growing the cells number until the overall mesh is sufficiently refine so that additional refinement does not change results. Firstly, the mesh size effect was investigated to predict the independency of computational results related to the mesh size and the cells number, by generate eight kinds of meshes. Figure 4 shows the effect of grid cells number on the drag coefficient at velocity inlet of about 20 m/s. From this figure it can concluded that, using the CFD domain with cells number of about 3000000 will be best suitable for reducing the solution time with acceptable percentage of error. To verify the current numerical model, a similar model of a heavy truck was developed and examined with same boundary conditions and the computational results were

compared with experiment measurement data using three turbulence models like enhanced wall treatment Realizable k–ε, standard k–ω model, and Spalart-Allmaras model. The coefficient of drag (C_D) variation with the Reynolds number was plotted on the same graph with same axes-scale as shown in Figure 5. The obtained results show that a good agreement of computational results with the corresponding results of the experimental measurement data. From Figure 5, it is found that the computational results which obtained using Realizable k– ε model of turbulence have more accuracy than computational results obtained using k–ω and Spalart-Allmaras models with a maximum percentage error of about 7.5%.

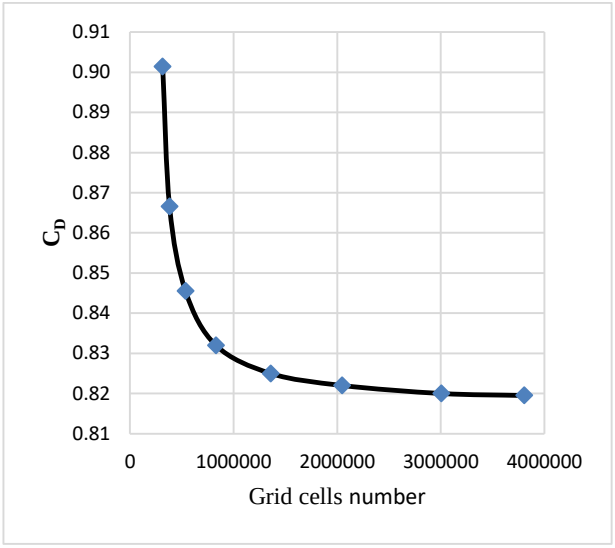

Fig. 4. Coefficient of drag against number of grid cells at velocity inlet 20 m/s

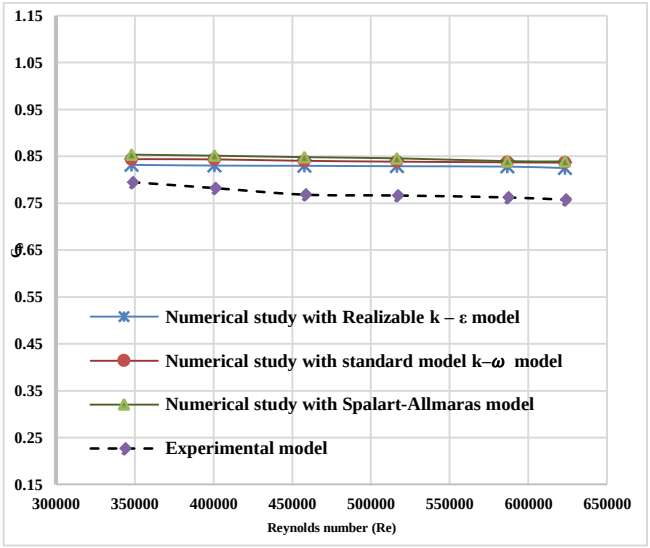

Fig. 5. Drag coefficient comparison of the standard 3D truck for different turbulence models

3. Profile Modification

The drag reduction devices and the truck profile modification were described using several geometric parameters as shown in Figure 6. These parameters are the front fillet radius ratio (FFRR), the mid fillet radius ratio (MFRR), the top fillet radius ratio (TFRR), the cab truck angle ratio (CTAR), the gap length device ratio (GLDR), the flat flap angle ratio (FFAR), the flap length ratio (FLR), and flap area ratio (FAR) as shown in Figure 6 (a, b, c, d, e, f, g, and h) respectively.

The parameter description and it is operation range were summarized in Table 1. Finally, at the air free stream velocity of about 20m/s, the standard truck profiles were tested without and with the drag reduction modifications devices and then compare between them to investigate the percentage improvement of drag reduction ratios.

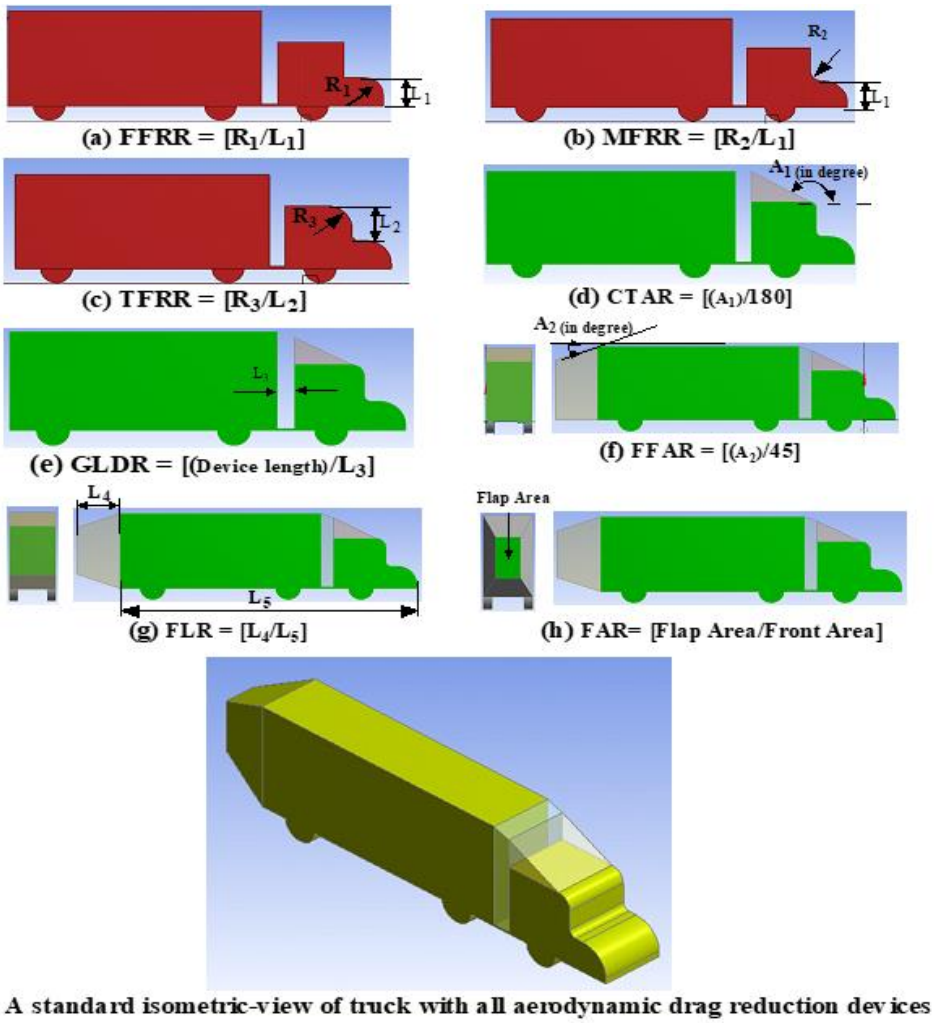

Fig. 6. Drag reduction devices and the truck profile modification

Table 1
Profile modification parameters description and operation range

Parameter	Description	Range
FFRR	Is the ratio of fillet radius to the height of front cabin (R_1/L_1)	0, 0.2, 0.4, 0.58, 0.8
MFRR	Is the ratio of mid fillet radius to the height of front cabin (R_2/L_1)	0, 0.2, 0.4
TFRR	Is the ratio of top fillet radius to the height of top front cabin (R_3/L_2)	0, 0.2, 0.3, 0.6, 0.8
CTAR	Is the ratio of cap truck angle over to 180° ($A_1/180°$) which added above the truck carbine	0.805, 0.833, 0.861, 0.889, 0.916
GLDR	Is the ratio of gap length device over total gap length (Device length/L_3)	0, 0.5, 1
FFAR	Is the ratio of flat flap angle over 45° ($A_2/45°$)	0.111, 0.222, 0.333, 0.444, 0.667
FLR	Is the ratio of the flat flap length to the total length of truck (L_4/L_5)	0.0478, 0.1196, 0.1914 with FFAR of about 0.333
FAR	Is the ratio of flap area to the front of container of the truck (flap area / front area)	0.25, 0.56, 0.75 with constant FLR

4. Experimental Setup

4.1 Wind Tunnel

To validate the computational results which examined in the previous computational sections, the aerodynamic characteristics of standard truck model that equipped with different drag reduction devices were tested. For performed these tests, a standard truck model was manufactured with the same geometry and dimensions that used in computational model calculations. The coefficient of drag was measured for different profiles modifications by using open-circuit suction wind tunnel of the aerodynamics laboratory of the institute of aviation engineering and technology, Egypt, as shown in Figure 7. The experimental data measured by wind tunnel were compared with numerical results which obtained from computational solution and the percentage error between them were determined.

Fig. 7. Truck model inside the test section of wind tunnel of aerodynamics laboratory

4.2 Water Tunnel

The water tunnel is considered an essential device which using to observing any hydrodynamic behaviour of the submerged bodies in the water flow. It is also used in examination the flow behaviour over numerous structures and analysing the flow property across boundary layer (i.e., flow separation, vortex shedding etc.) creates it more valuable additional counterpart facilities. In this study, low-speed water flow tunnel of the irrigation laboratory of the institute of aviation engineering and technology, Egypt, was used to visualize the aerodynamic behaviour, vortex formations and streamlines around the standard heavy truck as shown in Figure 8. This tunnel has speed range of about 0: 6 m/s and test section dimensions of (WHL) 0.5 x 1 x1.5 meters.

Fig. 8. Water tunnel experimental setup

5. Results

5.1 Computational Results

The profiles modification of a standard truck with variable dimensions of drag reduction devices were design using DESIGN MODULAR of ANSYS FLUENT program. The computational domain meshing was performed, the boundary conditions are defined, and the operation conditions are setting. The speed of vehicle is assumed to have of about 20m/s (R_e = 575321) at ambient air standard condition. The air temperature, density, static pressure, and the coefficient of viscosity are about 300K, ρ=1.225kg/m^3, 101325Pa, and μ=1.7894×10^{-5}kg/m.s respectively. To predict the effect of each truck profile modifications on the improvement of the aerodynamic drag reduction characteristics, the pressure, velocity, and turbulence kinetic energy contours were investigated, and the streamlines were plotted around the truck profile.

5.1.1 Pressure contour

The distribution of pressure contours around the truck body were investigated without and with using the aerodynamic drag reduction as shown in Figure 9. From Figure 9(a), it is notice that a non-uniform distribution in pressure across truck body and the areas of high-intensity of pressure (stagnation points) are located at the front surface of cabin, container, and wheels of truck which leads to increasing the force of drag on the overall truck body. Figure 9(b) illustrate the variation of pressure contours in case of truck with drag reduction devices. From Figure 9(b), it is noticing the distribution of pressure across truck body is more uniform compared to the case of truck without any devices of drag reduction as shown in Figure 9(a). The areas of high-intensity of pressure (stagnation points) are located only at the front surface of cabin, and wheels of truck. Also, we can note that the pressure intensity was decrease at the truck container which leads to decreasing in the overall force of drag on truck body.

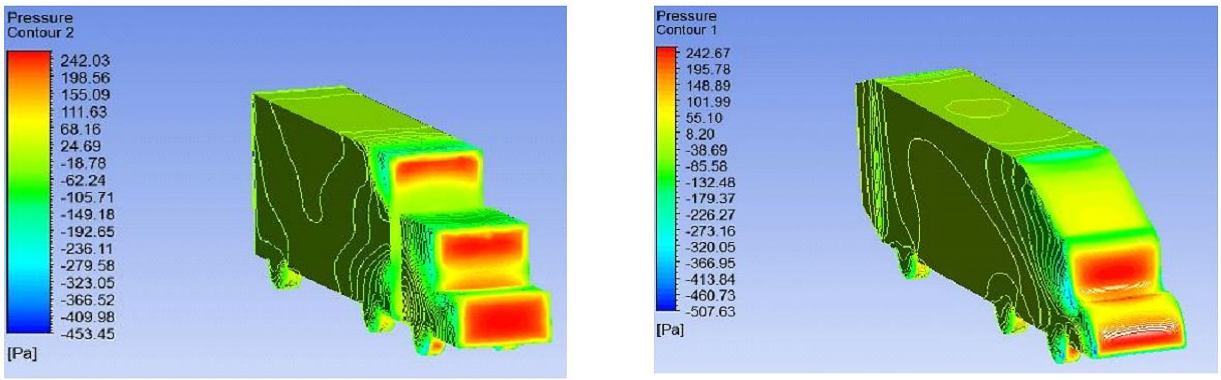

(a) (b)

Fig. 9. Pressure contour around truck (pa) (a) Without drag reduction devices, (b) With all drag reduction devices

5.1.2 Velocity contour

The distribution of velocity contours and vectors of velocity around the truck body were investigated without and with using the aerodynamic drag reduction as shown in Figure 10. From Figure 10(a), it is notice that the regions that have high-intensity of flow recirculation are located at front surface of the cabin, above the container, and back the container due to the sharp edges in these areas which finally leads to increasing the overall force of drag on truck body. Figure 10(b) illustrate the variation of velocity contours and vectors in case of truck with drag reduction devices. From Figure 10(b), it is noticing generally the separation intensity was decreased totally around truck compared to the case of truck without devices of drag reduction as shown in Figure 10(a) which finally leads to decreasing in the overall force of drag on truck body.

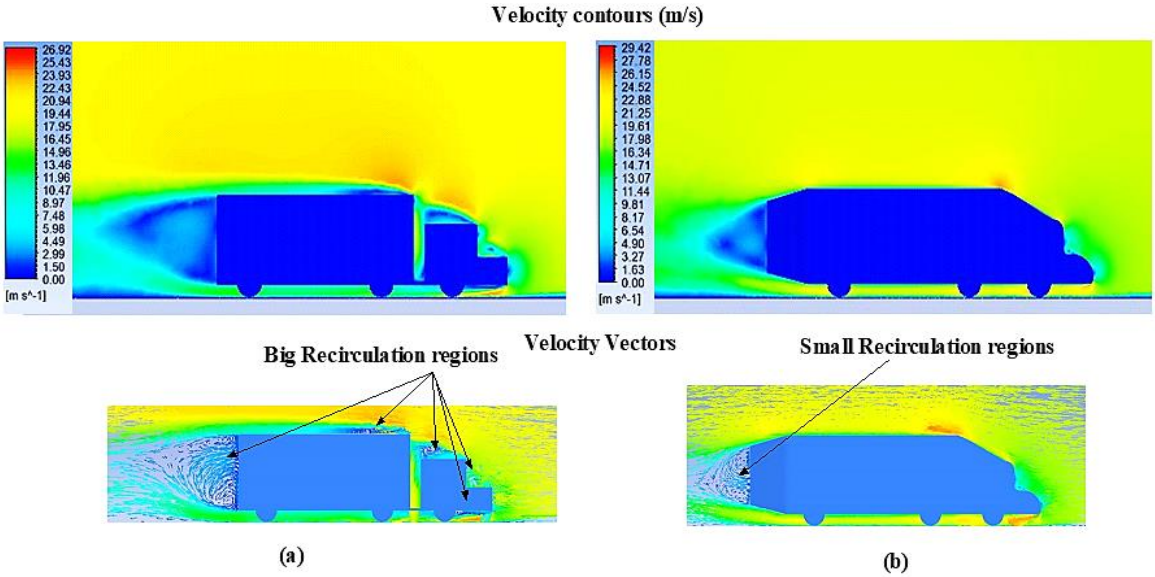

Fig. 10. Velocity contours and vectors around truck (a) Without drag reduction devices (b) With all drag reduction devices

5.1.3 Turbulence kinetic energy contours

The distribution of turbulence kinetic energy contours around the truck body were investigated without and with using the aerodynamic drag reduction as shown in Figure 11. From Figure 11(a), it

is notice that the high turbulence kinetic energy was observed at front of cabin, above the cabin surface, in the gap between cabin and container, above the container and at rear of container. This high turbulence causes turbulent eddies formation because of the high gradient of adverse pressure and the separation of flow that occur near the edges. Figure 11(b) illustrate the variation of turbulence kinetic energy contours around truck profile in case of truck with drag reduction devices. From Figure 11(b), it is observed that the flow around truck body was smoothing, the turbulence and wake formation are decreased because of using the drag reduction devices which finally leads to decreasing in the overall force of drag on truck body.

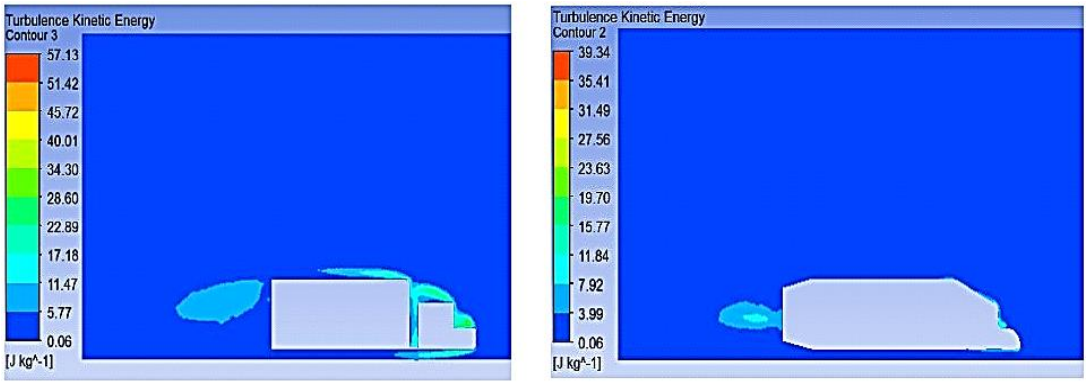

(a) (b)

Fig. 11. Turbulence Kinetic Energy around truck (a) Without drag reduction devices (b) With all drag reduction devices

5.1.4 Streamlines behavior

Here, to predict the strength of vortex formations effect and the critical locations of it, the distribution of streamlines around the truck body were investigated without and with using the aerodynamic drag reduction as shown in Figure 12. From Figure 12(a), it is notice that a non-uniform and random streamlines air flow were observed at front of cabin, above the cabin, in the gap between cabin and container, above the container and at rear of the container. This behaviour of flow leads to generate a big recirculation of air flow at these regions. Figure 12(b) illustrate the variation of turbulence kinetic energy contours around truck profile in case of truck with drag reduction devices. From Figure 12(b), it is observed that the recirculation is very small, the air flow is more uniform and aligned to the truck surface. This behaviour of flow leads to decreasing drag coefficient on the overall truck body.

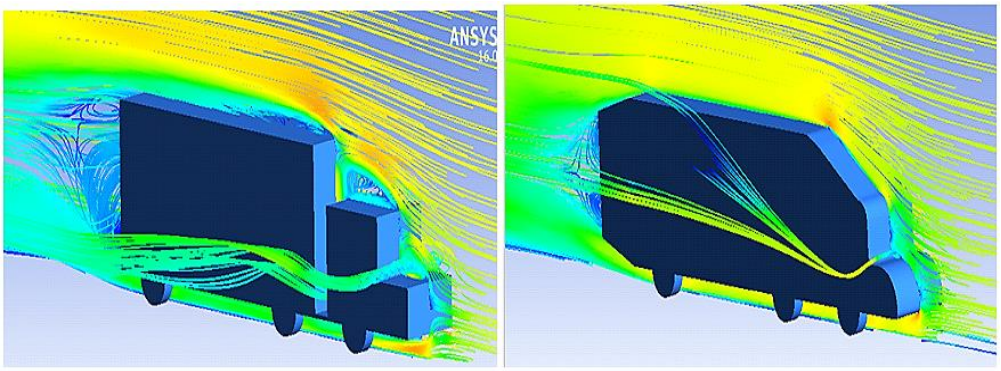

(a) (b)

Fig. 12. 3D streamlines around truck (a) Without drag reduction devices (b) With all drag reduction devices

5.2 Effect of Different Profiles Modification's on Drag Coefficient Improvement

To investigate the effect of different drag reduction devices on the improvement of the coefficient of drag of the heavy truck, the coefficient of drag was investigated without and with using the aerodynamic drag reduction devices. Firstly, for the truck without any modification's profiles, it is found the coefficient of drag is about 0.8283.

5.2.1 Effect of front fillet radius ratio of cabin (FFRR)

Figure 13 show the variation of drag coefficient (C_D) of a standard truck model for different FFRR. From this figure, it is notice that the coefficient of drag is decreasing gradually as the FFRR increasing. The decreasing in coefficient of drag mainly due to decreasing the recirculation in the front of truck. Generally, this behaviour of flow leads to decreasing coefficient of drag on overall truck body. From Figure 13, it can conclude that the minimum value of drag coefficient is about 0.7082 which occurs at FFRR= 0.8 and the percentage improvement is about 17%.

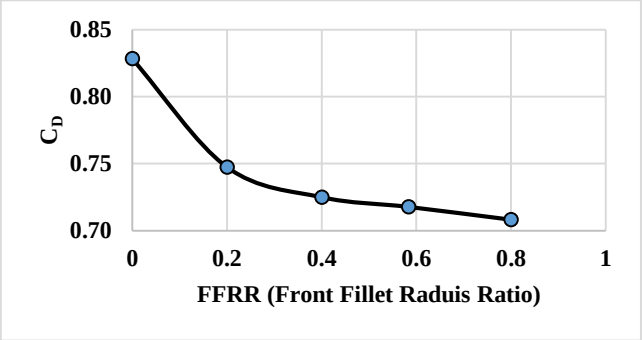

Fig. 13. Drag coefficient (C_D) variation with FFRR

5.2.2 Effect of mid fillet radius ratio (MFRR)

Figure 14 illustrate the variation of drag coefficient (C_D) of a standard truck model for different MFRR at constant FFRR = 0.8. From this figure, it is notice that as MFRR increasing the coefficient of drag is decreasing rapidly until reach to the minimum value and then return to increasing again after MFRR=0.2. The decreasing in coefficient of drag mainly due to decreasing the recirculation in the front of truck. Generally, this behaviour of flow leads to decreasing coefficient of drag on overall truck body. From Figure 14, it can conclude that the minimum value of drag coefficient is about 0.7035 which occurs at MFRR= 0.2 and the percentage improvement is about 18%.

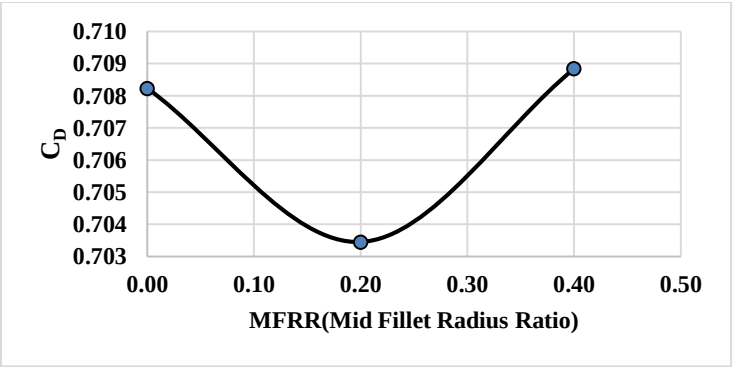

Fig. 14. Drag coefficient (C_D) variation with MFRR at FFRR=0.8

5.2.3 Effect of top fillet radius ratio (TFRR)

Figure 15 illustrate the variation of drag coefficient (C_D) of a standard truck model for different TFRR at constant FFRR = 0.8 and MFRR = 0.2. From this figure, it is notice that as TFRR increasing the coefficient of drag is increasing rapidly until reach to the highest value and then return to decreasing gradually again after TFRR=0.2. The increasing in coefficient of drag mainly due to Coandă effect that's increasing recirculation of flow above the container, shown in Figure 16. From Figure 15, it can conclude that the maximum value of drag coefficient is about 0.85 which occurs at TFRR= 0.2 and this leads to no improvement in the drag.

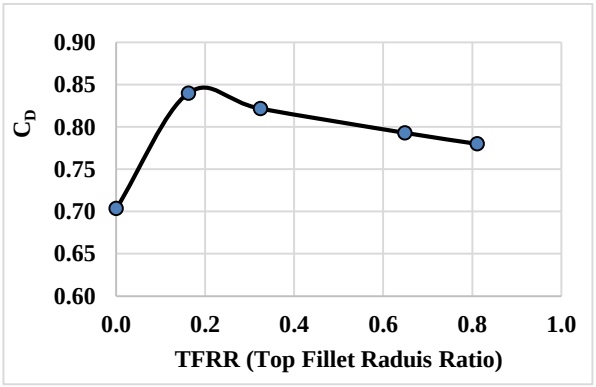

Fig. 15. Drag coefficient (C_D) variation with TFFR for FFRR =0.8 and MFRR =0.2

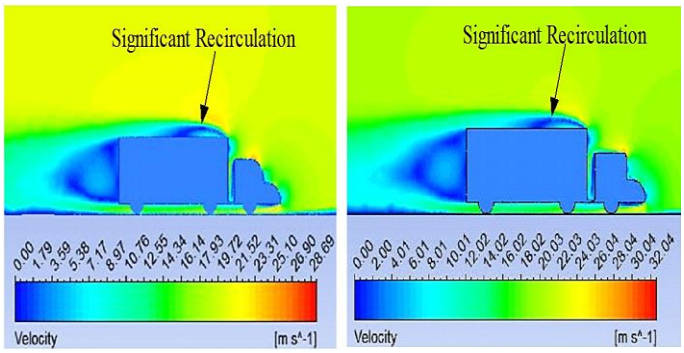

(a) (b)

Fig. 16. Velocity contours of truck model for FFRR=0.8 and MFRR=0.2, (a) TFRR=0.2, (b) TFRR=0.8

5.2.4 Effect of cab truck angle ratio (CTAR)

Figure 17 illustrate the variation of drag coefficient (C_D) of a standard truck model for different CTAR, TFRR at constant FFRR = 0.8 and MFRR = 0.2. From this figure, it is notice that for all vales of TFRR as CTAR increasing the coefficient of drag is decreasing rapidly until reach to the minimum value and then return to increasing gradually again. Also, it is observed that the corresponding CTAR value of the minimum coefficient of drag decreasing with increasing TFRR value. From Figure 17, it can conclude that the lowest minimum value of drag coefficient is about 0.6488 which occurs at TFRR= 0.2, CTAR = 0.861 (equivalent a cap truck angle of about 155 degrees) and this leads to improvement in the coefficient of drag by about of 26%. The vectors of velocity and the recirculation behaviours around truck body for TFRR = 0.2 and different CTAR are shown in Figure 18. From this figure, it is notice that the low strength of recirculation was obtained at the optimum cap truck angle but if this is angle is less than or exceeds the optimized value, the strength of recirculation is increasing rapidly, and a big recirculation appear in above and in front of truck which can cause an increasing in drag as illustrated in Figure 18(b, a, and c) respectively.

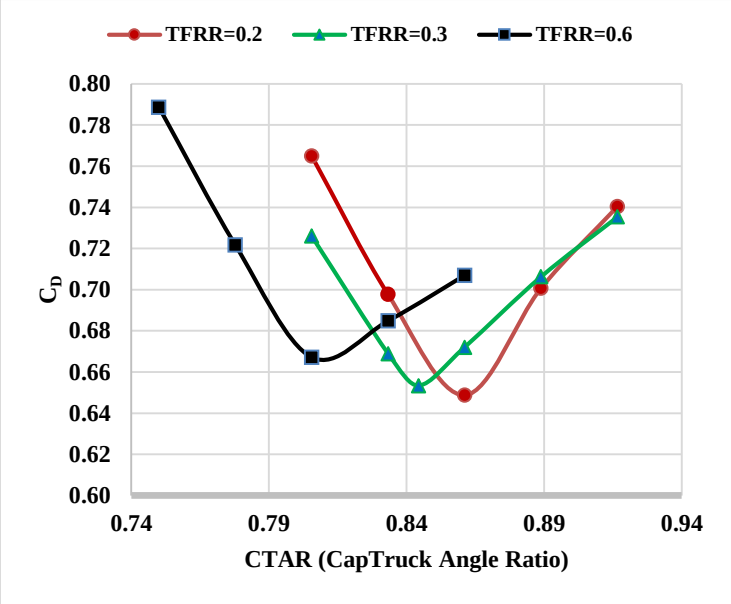

Fig. 17. Drag coefficient (C_D) variation with CTAR for FFRR = 0.8, MFRR = 0.2, and TFRR [0.2, 0.3, 0.6]

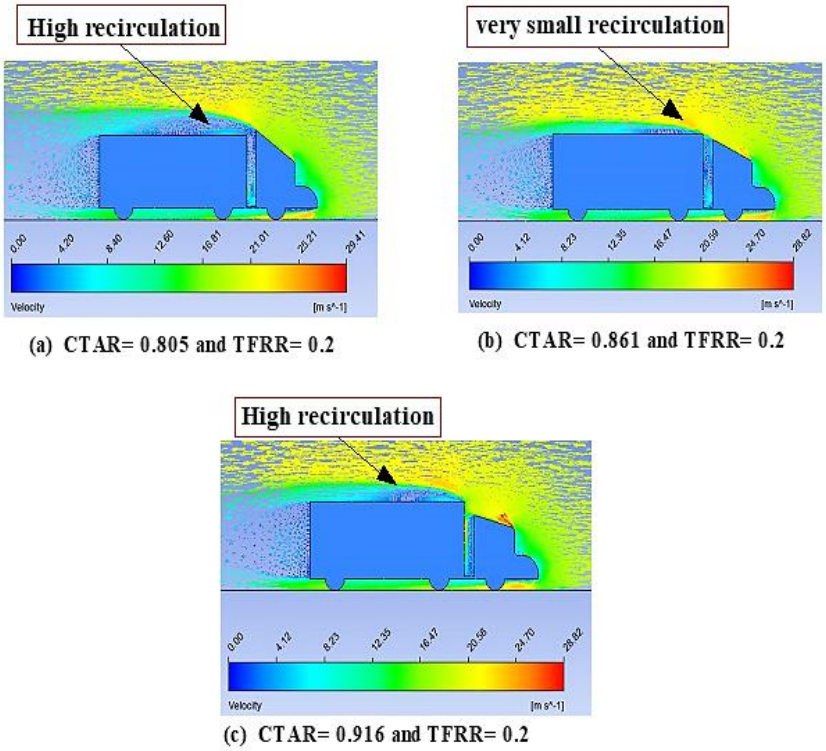

Fig. 18. Velocity vectors in (m/s) of standard truck model at FFRR=0.8, MFRR=0.2 and for different CTAR

5.2.5 Effect of gap length device ratio (GLDR)

Figure 19 illustrate the variation of drag coefficient (C_D) of a standard truck model for different GLDR at constant FFRR = 0.8, MFRR = 0.2, and CTAR = 0.861. From this figure, it is notice that the drag coefficient is decreasing gradually as the GLDR increasing. The decreasing in coefficient of drag mainly due to decreasing the recirculation at the gap between cabin and container. Generally, this behaviour of flow leads to decreasing coefficient of drag on overall truck body. From Figure 19, it can conclude

that the minimum value of the coefficient of drag is about 0.6089 which occurs at GLDR = 1 and the percentage improvement is about 35%.

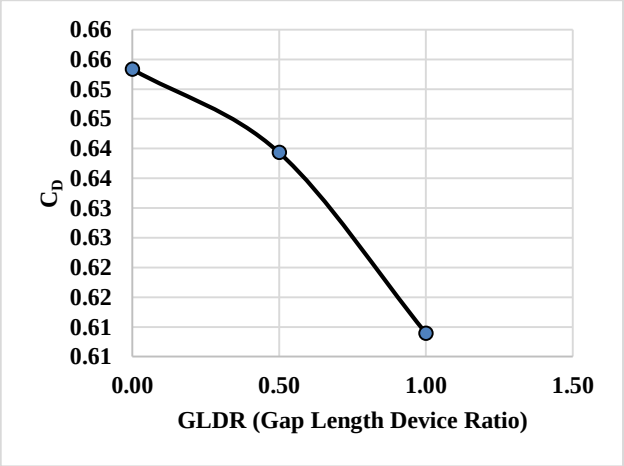

Fig. 19. Drag coefficient (C_D) variation with GLDR for FFRR = 0.8, MFRR = 0.2, TFRR 0.2, and CTAR = 0.833

5.2.6 Effect of flat flap angle ratio (FFAR)

Figure 20 illustrate the variation of drag coefficient (C_D) of a standard truck model for different FFAR at constant FFRR = 0.8, MFRR = 0.2, CTAR = 0.861 and GLDR= 1. From this figure, it is notice that as FFAR increasing the coefficient of drag is decreasing rapidly until reach to the minimum value and then return to increasing again after FFAR =0.35. Generally, this behaviour of flow leads to decreasing coefficient of drag on overall truck body. From Figure 20, it can conclude that the minimum value of drag coefficient is about 0.587 which occurs at FFAR =0.35 and the percentage improvement is about 40%.

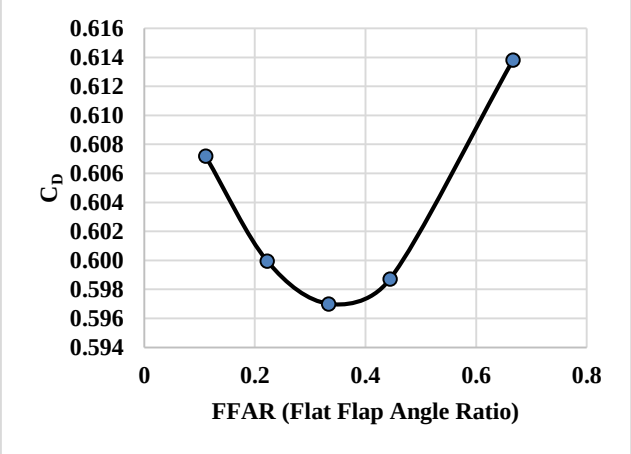

Fig. 20. Drag coefficient (C_D) variation with FFAR for FFRR = 0.8, MFRR = 0.2, TFRR 0.2, CTAR = 0.833, and GLDR= 1

5.2.7 Effect of flap length ratio [FLR]

Figure 21 illustrate the variation of drag coefficient (C_D) of a standard truck model for different FLR at constant FFRR = 0.8, MFRR = 0.2, CTAR = 0.861, GLDR= 1 and FFAR = 0.35. From this figure, it

is notice that the coefficient of drag is decreasing gradually to reach the minimum value as the FLR increasing. This decreasing in the coefficient of drag is mainly due to decreasing the recirculation behind the truck container with increasing the flap length as shown in Figure 22. Generally, this behaviour of flow leads to decreasing coefficient of drag on overall truck body. From Fig. 21, it can conclude that the minimum value of drag coefficient is about 0.5724 which occurs at FLR= 0.1914 and the percentage improvement is about 31%.

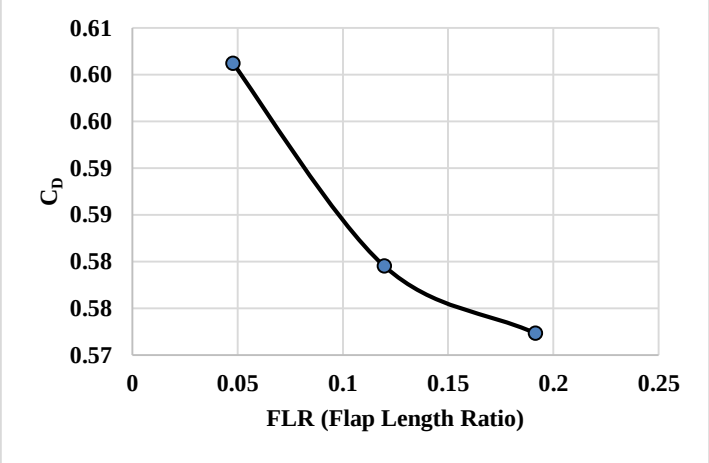

Fig. 21. Drag coefficient (CD) variation with FLR for FFRR = 0.8, MFRR = 0.2, TFRR 0.2, CTAR = 0.833, GLDR= 1, and FFAR = 0.333

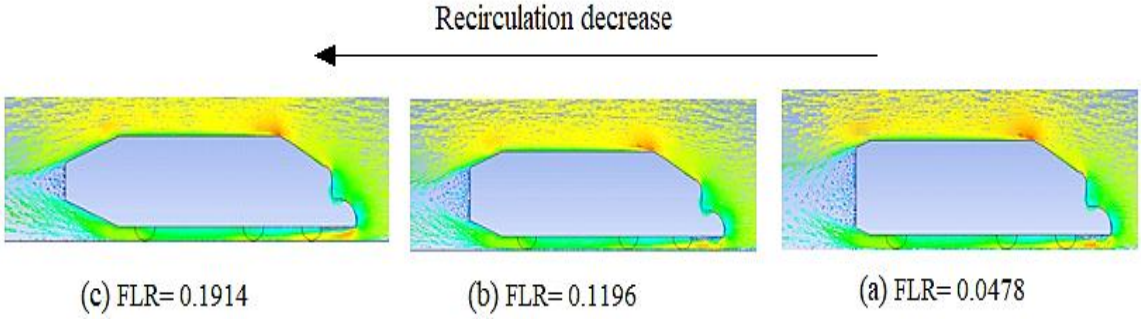

Fig. 22. Velocity vectors in (m/s) of standard truck model at FFRR=0.8, MFRR=0.2, TFRR=0.2, CTAR=0.833, GLDR=1 and FFAR= 0.333 and for different FLR

5.2.8 Effect of flap area ratio [FAR]

Figure 23 illustrate the variation of drag coefficient (C_D) of a standard truck model for different FAR at constant FFRR = 0.8, MFRR = 0.2, TFRR 0.2, CTAR = 0.861, GLDR= 1, FFAR = 0.35, and FLR=0.1914. From this figure, it is notice that the coefficient of drag is decreasing gradually as the FAR increasing. Generally, this behaviour of flow leads to decreasing coefficient of drag on overall truck body. From Figure 23, it can conclude that the minimum value of the coefficient of drag is about 0.52 which occurs at FLR=0.75 with percentage improvement is about 58%.

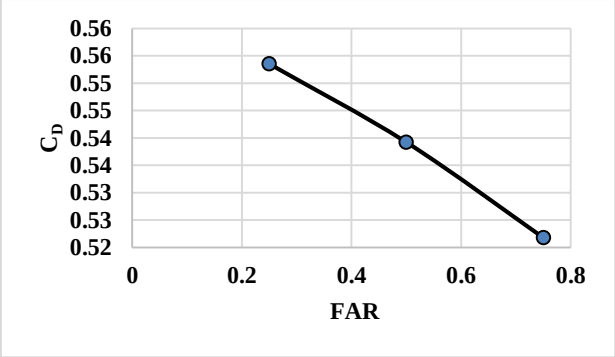

Fig. 23. Drag coefficient (C_D) variation with FAR for FFRR = 0.8, MFRR = 0.2, TFRR 0.2, CTAR = 0.833, GLDR= 1, FFAR = 0.333, and FLR=0.1914

5.3 Experimental Results

5.3.1 Flow visualization of water tunnel

In this study, two standard truck model were manufactured, one of them with all devices of drag reduction and the other model without any modifications. The coloured water was used to visualize the flow behaviours around the truck profile using the water tunnel as shown in Figure 24(a). Figure 24(b) illustrate the streamlines and vortex behaviour around the truck without any modifications. From this figure, it is show that, the vortex with high strength was observed at the front of cabin, above the cabin, gap between cabin and container, above the container and at rear of container. This behaviour of flow has compatible with the results of numerical study. Figure 24(c) illustrate the streamlines and vortex behaviour around the truck equipped with all aerodynamic drag reduction devices. From this figure, it is note that, the vortex recirculation is very small, the air flow is more uniform and aligned to surface of truck. This behaviour of flow has compatible with the results of numerical study and that is finally leads to decreasing the drag coefficient on the overall truck body.

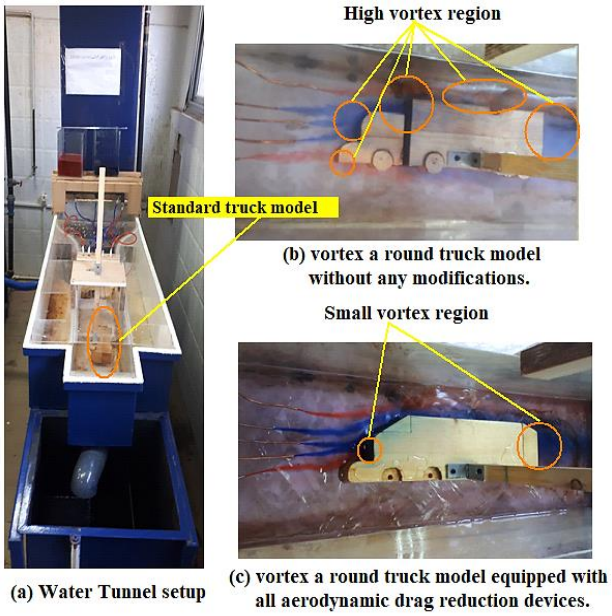

Fig. 24. Water tunnel experimental setup, (a) Water tunnel, Streamlines and vortex behaviour of truck model (b) Without any drag reduction devices, (c) With all drag reduction devices

5.3.2 Wind tunnel test

To predict the characteristics of drag, the model of truck was fixed in a closed jet test section of wind tunnel. The tunnel test section has a dimension of about 12 × 12- Inch and length of about 24-Inch with maximum velocity of about 108 mph. The force balance or table-mounted models was used to obtain a variety of aerodynamic measured data. The tunnel consisted with four major duct components. These components are the contraction cone, settling chamber, diffuser test section, and the fan housing, as shown in Figure 25. The wind tunnel's three-component sting balance is mounted on a parallelogram type model positioning system. At same time, the sting balance is used to measure two forces (drag, lift) and one moment. Finally, the indicated signals by sting balance are transformed to the inductor panel which convert the volt signals to forces, moment, pressure, and velocity. The blockage ratio of this model is about 3.5% within the acceptable blockage ratios are 5-7% in the closed jet test section. The ratio of the boundary layer thickness height at the centre of the test section compared to height of truck model is about of 0.08 at a velocity of about 20 m/s (R_e= 575321). The simplest technique is shown in Figure 26, where the test truck is simply elevated above the top of boundary layer that builds upon the bottom of wind tunnel's floor. While this seems like a rather simple solution, a boundary layer will still build upon the floor of the supporting platform, although this setup likely results in fewer adverse effects from boundary layer build-up than simply placing the test truck on the floor of the tunnel. At each tested cases, the measured data was collected and then averaged to minimizing the additional possible errors in the raw experimental data. The comparison between numerical results and experimental data for different modifications profiles and drag reduction devices were summarized in Figure 27. Finally, the experimental results show that a good agreement with the computational results with acceptable percentage error of about 5%.

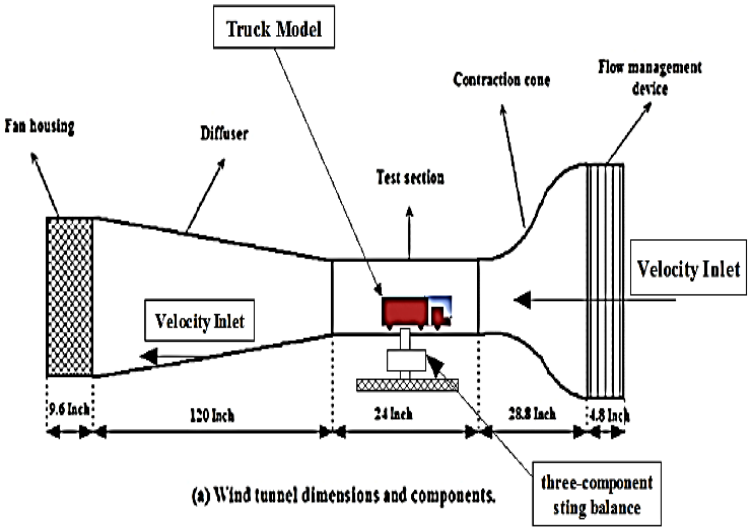

Fig. 25. Wind tunnel main component setup and dimensions

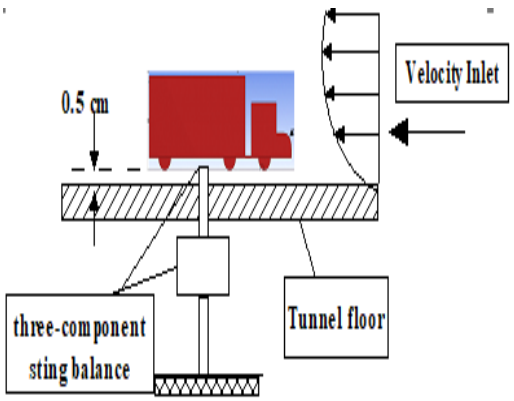

Fig. 26. A standard heavy truck test setup

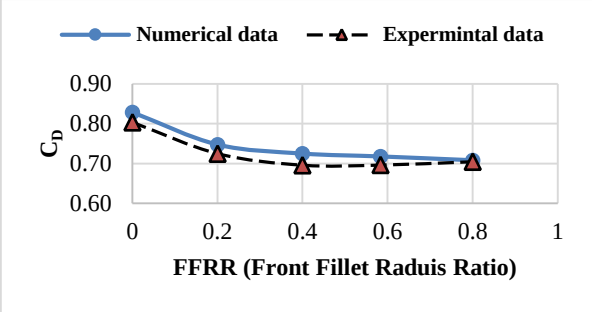

(a) Drag coefficient (C_D) variation with FFRR

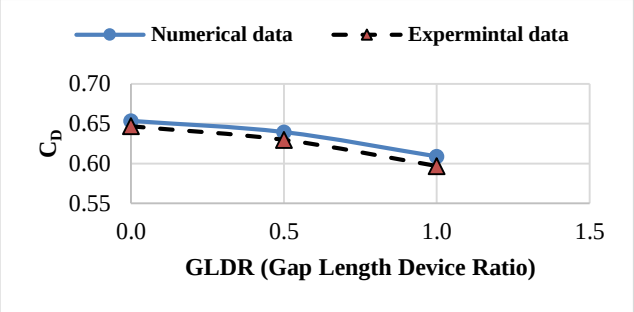

(e) Drag coefficient (C_D) variation with GLDR for FFRR = 0.8, MFRR = 0.2, TFRR 0.2, and CTAR = 0.833

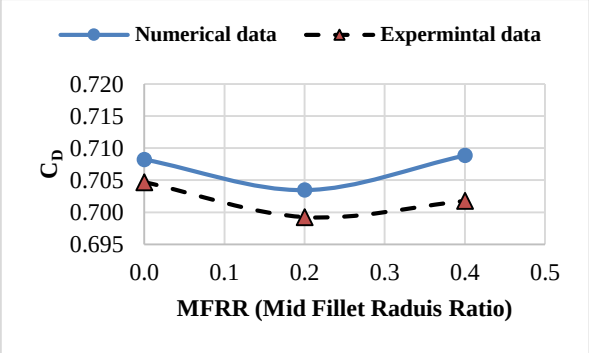

(b) Drag coefficient (C_D) variation with MFRR at FFRR=0.8

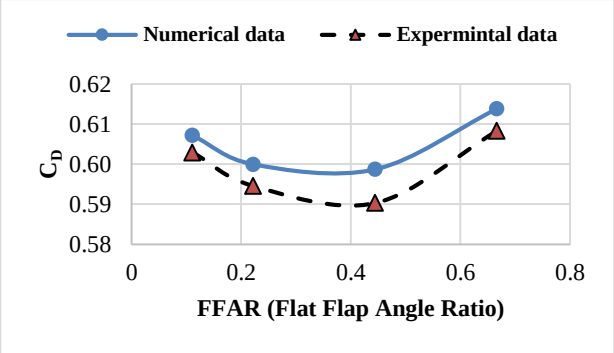

(f) Drag coefficient (C_D) variation with FFAR for FFRR = 0.8, MFRR = 0.2, TFRR 0.2, CTAR = 0.833, and GLDR= 1

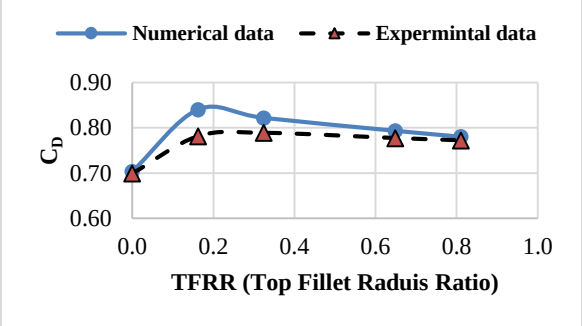

(c) Drag coefficient (C_D) variation with TFFR for FFRR =0.8 and MFRR =0.2

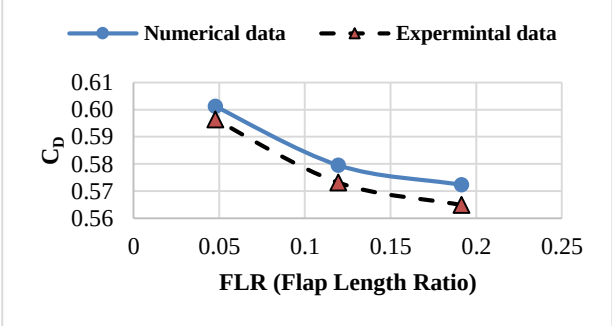

(g) Drag coefficient (C_D) variation with FLR for FFRR = 0.8, MFRR=0.2, TFRR=0.2, CTAR=0.833, GLDR= 1, and FFAR=0.333

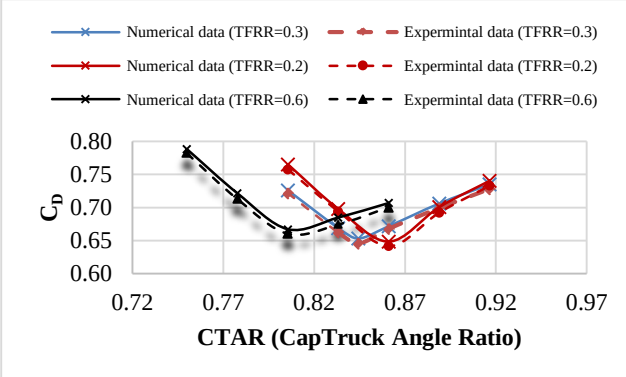

(d) Drag coefficient (C_D) variation with CTAR for FFRR = 0.8, MFRR = 0.2, and TFRR [0.2, 0.3, 0.6]

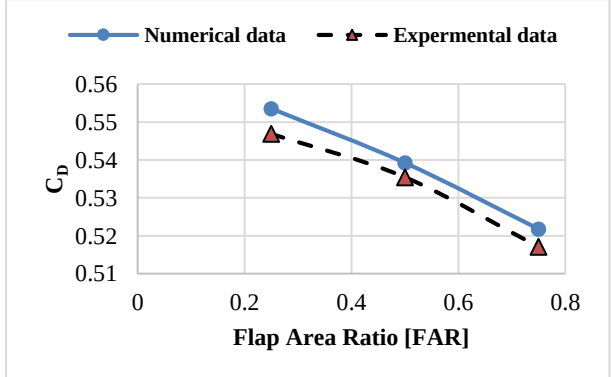

(h) Drag coefficient (C_D) variation with FAR for FFRR = 0.8, MFRR = 0.2, TFRR 0.2, CTAR = 0.833, GLDR= 1, FFAR = 0.333, and FLR=0.1914

Fig. 27. Comparison between numerical results and experimental data of standard truck model for different aerodynamic modifications profiles and drag reduction devices at velocity 20 m/s

6. Conclusions

Reducing the fuel consumption is considered one of the most significant objectives in several automotive development researches aiming to energy save, reduce the emissions, and hence, protecting the environment from the danger of global warming. Improving the aerodynamic performance and reduce the drag is considered one of the essential issues used in automotive industry to decrease the consumption of fuel especially in the heavy freight vehicles and trucks. In this work, various devices of drag reduction were added to improve the profiles of a heavy freight vehicles and the effects of each device were experimentally and computationally investigated. These additional devices are the front fillet radius ratio (FFRR), the mid fillet radius ratio (MFRR), the top fillet radius ratio (TFRR), the cab truck angle ratio (CTAR), the gap length device ratio (GLDR), the flat flap angle ratio (FFAR), the flap length ratio (FLR), and flap area ratio (FAR). A $1/50^{th}$ scale of a standard heavy truck were taken to construct the computational and experimental model. The drag coefficient, contours of turbulence kinetic energy, pressure, streamlines, velocity, velocity vectors were predicted with and without additional devices. In general, it is observed that, these attached devices have a notable impact on the aerodynamic drag reduction of the heavy vehicles and trucks. The obtained computational results show that, the front fillet radius and the mid fillet radius have a significant effect and reduce the drag coefficient by about 17%, 18% respectively. The top fillet radius profile without cap increases the coefficient of drag due to the Coandă Effect. When the top fillet radius was utilized combined with cap of truck, the coefficient of drag reduced by about 26%. Adding gap devices with various lengths reduce the coefficient of drag by about 35%. Adding the flat flap at rear of truck improve the coefficient of drag by about 40. The flap length and flap area red improve the coefficient of drag by about 45. Installing all supplementary parts with their optimized positions at the same time, help to reduce the drag coefficient by about 59 % compared with the truck without any profile's modifications. Finally, a model of truck was manufactured and tested in the open-circuit suction wind tunnel and the experimental results show a good agreement with the computational results with acceptable percentage error of about 5%.

Acknowledgement

The authors state that this research did not receive any specific grant from funding agencies in the public, commercial, or not-for-profit sectors.

References

[1] Odhams, A. M. C., R. L. Roebuck, Y. J. Lee, S. W. Hunt, and D. Cebon. "Factors influencing the energy consumption of road freight transport." *Proceedings of the Institution of Mechanical Engineers, Part C: Journal of Mechanical Engineering Science* 224, no. 9 (2010): 1995-2010. https://doi.org/10.1243/09544062JMES2004

[2] Williams, Susan E., Stacy Cagle Davis, and Robert Gary Boundy. "Transportation energy data book: Edition 36." *No. ORNL/TM-2017/513. Oak Ridge National Lab.(ORNL), Oak Ridge, TN (United States),* (2017). https://doi.org/10.2172/1878695

[3] Sarwani, Muhamad Khairul Ilman, Mas Fawzi, Shahrul Azmir Osman, and Wira Jazair Yahya. "Calculation of Specific Exhaust Emissions of Compression Ignition Engine Fueled by Palm Biodiesel Blend." *Journal of Advanced Research in Applied Sciences and Engineering Technology* 27, no. 1 (2022): 92-96. https://doi.org/10.37934/araset.27.1.9296

[4] Issaro, Assadawut, Piyanut Saengsikhiao, Juntakan Taweekun, and Wiriya Thongruang. "The Green Logistics Idea using Vacuum Insulation Panels (VIPs)." *Journal of Advanced Research in Fluid Mechanics and Thermal Sciences* 82, no. 2 (2021): 72-86. https://doi.org/10.37934/arfmts.82.2.7286

[5] Brogan, James J., Andreas E. Aeppli, Daniel F. Bagan, Austin Brown, Michael J. Fischer, Lance R. Grenzeback, Elaine McKenzie, Laura Vimmerstedt, Anant D. Vyas, and Erika Witzke. "Freight transportation modal shares: scenarios for a low-carbon future." *No. DOE/GO-102013-3705*. (2013). https://doi.org/10.2172/1338446

[6] Tilvaldyev, Shehret. "Review of Aerodynamic Drag Reduction Devices for Heavy Trucks and Buses." *Instituto de Ingeniería y Tecnología* (2020).

[7] Buckley Jr, Frank T., William H. Walston Jr, and Colin H. Marks. "Fuel savings from truck aerodynamic drag reducers and correlation with wind-tunnel data." *Journal of Energy* 2, no. 6 (1978): 321-329. https://doi.org/10.2514/3.62383
[8] Muirhead, Vincent U., and Edwin J. Saltzman. "Reduction of aerodynamic drag and fuel consumption for tractor-trailer vehicles." *Journal of Energy* 3, no. 5 (1979): 279-284. https://doi.org/10.2514/3.48005
[9] Cooper, Kevin Russell. "The wind-tunnel simulation of surface vehicles." *Journal of wind engineering and industrial aerodynamics* 17, no. 2 (1984): 167-198. https://doi.org/10.1016/0167-6105(84)90055-2
[10] Storms, Bruce, Dale Satran, James Heineck, and Stephen Walker. "A study of reynolds number effects and drag-reduction concepts on a generic tractor-trailer." In *34th AIAA Fluid Dynamics Conference and Exhibit*, (2004): 2251. https://doi.org/10.2514/6.2004-2251
[11] Tsuei, Lun, and Ömer Savaş. "Transient aerodynamics of vehicle platoons during in-line oscillations." *Journal of Wind Engineering and Industrial Aerodynamics* 89, no. 13 (2001): 1085-1111. https://doi.org/10.1016/S0167-6105(01)00073-3
[12] Howell, Jeff, Chris Sherwin, Martin Passmore, and Geoff Le Good. "Aerodynamic drag of a compact SUV as measured on-road and in the wind tunnel." *SAE Transactions* (2002): 583-590. https://doi.org/10.4271/2002-01-0529
[13] Schoon, Ronald E. "On-road evaluation of devices to reduce heavy truck aerodynamic drag." In SAE 2007 *Commercial Vehicle Engineering Congress & Exhibition*, no. 2007-01-4294. (2007). https://doi.org/10.4271/2007-01-4294
[14] Englar, Robert J. "Advanced aerodynamic devices to improve the performance, economics, handling and safety of heavy vehicles." *No. 2001-01-2072. SAE Technical Paper* (2001). https://doi.org/10.4271/2001-01-2072
[15] Choi, Haecheon, Jungil Lee, and Hyungmin Park. "Aerodynamics of heavy vehicles." *Annual Review of Fluid Mechanics* 46 (2014): 441-468. https://doi.org/10.1146/annurev-fluid-011212-140616
[16] Niknahad, Ali. "Numerical study and comparison of turbulent parameters of simple, triangular, and circular vortex generators equipped airfoil model." *Journal of Advanced Research in Numerical Heat Transfer* 8, no. 1 (2022): 1-18.
[17] Elsafty, Kareem Ahmed Ismail, Atif Mohamed Emad Elsherif, Ahmed Abdelhamid Ibrahim, Omar Sherif Mohamed, and Ahmed Mohamed Reda Elbaz. "Investigating the Performance of a Novel Multi-Element Airfoil Concept Using Numerical Analysis." *Journal of Advanced Research in Fluid Mechanics and Thermal Sciences* 97, no. 2 (2022): 126-145. https://doi.org/10.37934/arfmts.97.2.126145
[18] Ortega, J., K. Salari, A. Brown, and R. Schoon. "Aerodynamic drag reduction of class 8 heavy vehicles: a full-scale wind tunnel study." *No. LLNL-TR-628153. Lawrence Livermore National Lab.(LLNL), Livermore, CA (United States)*, (2013). https://doi.org/10.2172/1073121
[19] Choi, Haecheon, Jungil Lee, and Hyungmin Park. "Aerodynamics of heavy vehicles." *Annual Review of Fluid Mechanics* 46 (2014): 441-468. https://doi.org/10.1146/annurev-fluid-011212-140616
[20] Coon, J. D., and K. D. Visser. "Drag reduction of a tractor-trailer using planar boat tail plates." In *The Aerodynamics of Heavy Vehicles: Trucks, Buses, and Trains*, (2004): 249-265. https://doi.org/10.1007/978-3-540-44419-0_24
[21] BROWAND, Fred, Charles RADOVICH, and Mathieu BOIVIN. "Fuel savings by means of flaps attached to the base of a trailer: Field test results." *SAE transactions* 114, no. 6 (2005): 1172-1186. https://doi.org/10.4271/2005-01-1016
[22] Cooper, Kevin R. "The wind tunnel testing of heavy trucks to reduce fuel consumption." *SAE transactions* (1982): 4118-4130. https://doi.org/10.4271/821285
[23] Mohamed-Kassim, Zulfaa, and Antonio Filippone. "Fuel savings on a heavy vehicle via aerodynamic drag reduction." *Transportation Research Part D: Transport and Environment* 15, no. 5 (2010): 275-284. https://doi.org/10.1016/j.trd.2010.02.010
[24] Mosaddeghi, Farshid, and Majid Oveisi. "Aerodynamic drag reduction of heavy vehicles using append devices by CFD analysis." *Journal of Central South University* 22, no. 12 (2015): 4645-4652. https://doi.org/10.1007/s11771-015-3015-7
[25] Hyams, Daniel G., Kidambi Sreenivas, Ramesh Pankajakshan, D. Stephen Nichols, W. Roger Briley, and David L. Whitfield. "Computational simulation of model and full scale Class 8 trucks with drag reduction devices." *Computers & Fluids* 41, no. 1 (2011): 27-40. https://doi.org/10.1016/j.compfluid.2010.09.015
[26] Chilbule, Chaitanya, Awadhesh Upadhyay, and Yagna Mukkamala. "Analyzing the profile modification of truck-trailer to prune the aerodynamic drag and its repercussion on fuel consumption." *Procedia Engineering* 97 (2014): 1208-1219. https://doi.org/10.1016/j.proeng.2014.12.399
[27] AbdelGhany, E. S. "CFD Investigation for Effect of the Aerodynamic Truck - Cabin Profiles and Devices on the Truck Performance." *IJENS* (2020): 1-17.
[28] Gilhaus, A. "The influence of cab shape on air drag of trucks." *Journal of Wind Engineering and Industrial Aerodynamics* 9, no. 1-2 (1981): 77-87. https://doi.org/10.1016/0167-6105(81)90079-9
[29] Drollinger, R. A. "Heavy duty truck aerodynamics. SAE Tech Pap." (1987). https://doi.org/10.4271/870001

[30] Cooper, Kevin R. "Truck aerodynamics reborn-lessons from the past." *SAE transactions* (2003): 132-142. https://doi.org/10.4271/2003-01-3376
[31] Leuschen, Jason, and Kevin R. Cooper. "Summary of full-scale wind tunnel tests of aerodynamic drag-reducing devices for tractor-trailers." *The aerodynamics of heavy vehicles II: trucks, buses, and trains* (2009): 451-462. https://doi.org/10.1007/978-3-540-85070-0_41
[32] Garry, K. P. "Development of container-mounted devices for reducing the aerodynamic drag of commercial vehicles." *Journal of Wind Engineering and Industrial Aerodynamics* 9, no. 1-2 (1981): 113-124. https://doi.org/10.1016/0167-6105(81)90082-9
[33] Watkins, S., J. W. Saunders, and P. H. Hoffmann. "Comparison of road and wind-tunnel drag reductions for commercial vehicles." *Journal of Wind Engineering and Industrial Aerodynamics* 49, no. 1-3 (1993): 411-420. https://doi.org/10.1016/0167-6105(93)90035-M
[34] Garry, K. P. "A review of commercial vehicle aerodynamic drag reduction techniques." *Proceedings of the Institution of Mechanical Engineers, Part D: Transport Engineering* 199, no. 3 (1985): 215-220. https://doi.org/10.1243/PIME_PROC_1985_199_159_01
[35] Ingram, K. C. "The wind-averaged drag coefficient applied to heavy goods vehicles." In *Australian Road Research Board Symposium*, *no. Supp. Report 392* (1978).
[36] McCallen, Rose C., Kambiz Salari, Jason M. Ortega, Larry J. DeChant, Basil Hassan, Christopher J. Roy, W. David Pointer et al. "DOE's Effort to Reduce Truck Aerodynamic Drag–Joint Experiments and Computations Lead to Smart Design." In *34th AIAA Fluid Dynamics Conference and Exhibit* (2004): 2249. https://doi.org/10.2514/6.2004-2249
[37] Khaled, Mahmoud, Hicham El Hage, Fabien Harambat, and Hassan Peerhossaini. "Some innovative concepts for car drag reduction: A parametric analysis of aerodynamic forces on a simplified body." *Journal of wind engineering and industrial aerodynamics* 107 (2012): 36-47. https://doi.org/10.1016/j.jweia.2012.03.019
[38] Cooper, Kevin R. "Commercial vehicle aerodynamic drag reduction: historical perspective as a guide." In *The Aerodynamics of Heavy Vehicles: Trucks, Buses, and Trains*, (2004): 9-28. https://doi.org/10.1007/978-3-540-44419-0_2
[39] Schito, Paolo. "Numerical and experimental investigation on vehicles in platoon." *SAE International Journal of Commercial Vehicles* 5, no. 2012-01-0175 (2012): 63-71. https://doi.org/10.4271/2012-01-0175
[40] Khalil, Essam E., Osama E. Abdelattif, Eslam S. AbdelGhany, and Gamal A. ElHariri. "Computational Analyses of Aerodynamic Characteristics of NACA653218airfoil." In *54th AIAA Aerospace Sciences Meeting*, (2016): 1367. https://doi.org/10.2514/6.2016-1367